Pedogenic processes and clay transformations in bisequal soils of the southern taiga zone

PEDOGENIC PROCESSES AND CLAY TRANSFORMATIONS IN BISEQUAL SOILS OF THE SOUTHERN TAIGA ZONE.

Eleonora Bonifacio[a], Gloria Falsone[a], Gennady Simonov[b], Tatiana Sokolova[c] and Inna Tolpeshta[c]

[a] Università di Torino, DIVAPRA, via L. da Vinci 44, Torino, 10095, Italy.
[b] Institute of Biology of Komi Scientific Centre, Ural Division RAS, Dept. of Soil Science, Kommunisticheskaya 28, Syktyvkar, Komi Republic, 167982, Russian Federation.
[c] Moscow Lomonosov State University, Vorob'evy Gori, Moscow, 199899, Russian Federation.

Corresponding author: Eleonora Bonifacio, E mail: Eleonora.bonifacio@unito.it

ABSTRACT

In bisequal soils a complex combination of pedogenic processes has occurred and the minerals that arise from a specific soil forming process may have been modified by other processes. In this work we investigated the mineralogical composition of the clay fraction and related it to pedogenic processes in three soils of the Russian Taiga. The soils showed evidences of clay translocation, podzolisation, and gleying with different intensities and combinations. Clay translocation was present in all profiles, but better expressed in profile 2. Evidences of podzolisation were found in profiles 2 and 3, but in this latter hydromorphic processes have also occurred. In profile 1 almost permanent water stagnation has lead to the development of a thick sphagnum cover. In all profiles, during the formation of the Alfisol sequa, the transformation of illite into vermiculite or smectite has occurred through the formation of mixed-layered minerals while the pH favoured Al-intercalation in the interlayer. When podzolisation started, the presence of HIV/HIS in the E horizon was no longer favoured, because of Al complexation by organic acids, but in the Bs horizons Al-intercalation in the interlayers continued, thus prolonging a mineralogical process that has started during the previous pedogenic phase. The formation of swelling minerals was moderate and related to the cheluviation phase of podzolisation. We found swelling mixed layer minerals only in the surface horizons of profile 1 and 3, where the vegetation cover was favourable to the production of aggressive organic acids and thus Al may be removed also from the structural sites of phyllosilicates. The reducing conditions acted upon soil minerals, but affected directly only Fe oxi(hydr)oxides. The dissolution of the protective Fe-films from mineral surfaces has, however, favoured the physical disintegration of feldspar grains where the waterlogging conditions were almost permanent.
Key words: clay illuviation, clay mineralogy, gleying, podzolisation, Russia.

INTRODUCTION

Bisequal soils are rather common in the Russian Taiga where Glossocryalfs border on Spodosols, and thus at the interface between the two soil types podzolisation is frequently found (Deckers, 2001). The Orthod profile typically develops in the eluvial horizon of the loamy Glossocryalf profile. Therefore, in addition to the transformations that have occurred during Alfisol development, the soil solid phase in the top horizons is affected also by the transformations which are typical of podzolisation.

Clay minerals are frequently used as indicators of pedogenesis as the mineralogy of the clay fraction is related to the pedogenic processes that have occurred in the soil, but clay minerals arising from the most recent process may have formed from those originated during the previous ones.

During Alfisol formation, the transformations of the clay phases are governed by the mobility of the elements released by mineral dissolution (Chesworth, 1992). Illite typically weathers to vermiculite through the release of potassium from the interlayer; the intercalation of Al hydroxyl-polymers often occurs, giving rise to hydroxy-interlayered vermiculites (HIV), and to pedogenic chlorites as the end members of the transformation (Allen and Hajek, 1989). Detrital chlorite tends to disappear by weathering to vermiculite (Banfield and Murakami, 1998), or smectite (Arocena and Sandborn, 1999) and, in both cases, the formation of mixed layer clay minerals between the two end members is common (e.g. Churchman, 1980; Środoń, 1999). Kaolinite has been reported as originating from almost all primary minerals (Wilson, 2004), but is typically pedogenic only in Oxisols and Ultisols, while in Cryalfs and Udalfs, its distribution is generally uniform with depth (Allen and Hajek, 1989), suggesting inheritance from the parent material.

In addition to the mineral transformations occurring via leaching of cations, some specific transformations occur during podzolisation. In the E horizons of sandy Spodosols swelling

minerals are commonly present, but their abundance increases with increasing intensity of podzolisation (Egli et al., 2004). The strong acidity favours chlorite dissolution (Ross, 1969; Bain and Duthie, 1984) and the presence of complexing organic agents enhances the removal of the Al polymers from the interlayer of vermiculites and smectites (e.g. Egli et al., 2003). In the Bs horizons, the mineralogical transformations are normally less marked (Righi et al., 1999), and both swelling and non-swelling minerals have been reported (e.g. Egli et al., 2004; Kitagawa, 2005).

Besides podzolisation and lessivage, additional processes may be present. In the taiga soils, the texture of the Spodosol sequum is typically finer than in the sandy Spodosols. Thus, an additional pedogenic process that often induces an even more complex soil profile is linked to hydromorphic conditions. They may develop in small depressions because of climatic conditions, but also on vast areas with impeded drainage, and lead to additional soil features and to transformations of the clay phase caused by redox processes. The reductive processes associated to hydromorphism have a direct effect on the solubilisation of Fe and Mn oxides and hydroxides, but may affect also layer silicates through a variation in their charge, thus influencing the CEC, the swelling behaviour and all properties associated to electrostatic interactions (Stucki, 2006).

In unmanaged situations waterlogging may in turn induce the development of Sphagnum layers and a general tendency to the formation of peatland. Sphagnum layers release leachates with high dissolved organic carbon contents, and a high proportion of organic acids (David and Vance, 1991). As organic acids affect silicate dissolution mainly through complexation (e.g. Robert and Berthelin, 1986), an enhancement of weathering of all aluminium silicates is expected.

The purpose of this work was to evaluate the pedogenic processes, and their intensity, in three bisequal soils of the Russian Southern Taiga zone, and to assess the transformations that have occurred to clay minerals because of soil processes.

MATERIALS AND METHODS

Study sites

The study area is located in the Central Forest State Biosphere Reserve of the Russian Federation, 56° 26’ - 56° 31’ N, 32° 29’ - 33° 01’ E, 250 km north-northwest of Moscow, in the Southern Taiga ecosystem zone (Figure 1). The Central Forest State Biosphere Reserve lies on a plateau of Paleozoic rocks, covered by a thick layer of Quaternary deposits (20-40 m), mainly originated by the mid-Pleistocene Moscow (Riss) glaciation. The relief is represented by end moraine ridges composed of brown and red-brown loams, and moraine plains with kames and kame terraces. Fluvioglacial sandy deposits ranging in thickness from 1.5 to 6 m are also common. Approximately 100 thousand years ago the last Valdai (Würm) glacial age began, and finished 17-20 thousand years ago. The age of the glacial deposits within the studied area is uncertain, as the exact determination of the southern boundary of the Valdai ice-sheet has not yet been established (Puzachenko et al, 2007). The glacial deposits were covered with loams and sandy loams of aeolian origin formed in the periglacial zone. Therefore, the soil parent material of the studied area is represented by poorly sorted loamy and clay loamy moraine deposits, usually red-coloured, covered by brown well-sorted loams and sandy loams. Lithologic discontinuities are hence rather common in the soils of area. The surface is moderately dissected, and ranges from flat to gently undulating plains. The climate is cool to cold with a mean annual temperature of +4°C, and a mean annual precipitation of 731 mm.

Three sites were selected, where pits were opened and soil profiles described. The vegetation is dominated by Norway spruce at site 1 and 3, while at site 2 spruce is associated with several species of broadleaves. Sphagnum was present at site 1, but absent at the other two sites. Soil samples were taken from each genetic horizon, air dried and passed through a 2 mm sieve.

Soil chemistry and mineralogy

The pH was determined in a 1:2.5 soil/distilled water suspension, the cation exchange capacity (CEC) using the $BaCl_2$-triethanolamine method (Rhoades, 1982) and the exchangeable bases were measured by atomic absorption spectrophotometry (AAS, Perkin Elmer 3030). The C and N contents were determined through dry combustion (CE Instruments NA2100 elemental analyser); the particle size distribution was evaluated by the pipette method after dispersion of the sample with Na-hexametaphosphate. The coarse sand content (2-0.2 mm) was also determined after pre-treating the samples with 30% H_2O_2 at 50°C, until foaming has stopped (Gee and Bauder, 1986). The pedogenic iron oxide content (Fe_D) was evaluated by the Na dithionite-citrate-bicarbonate extraction (Mehra and Jackson, 1960) at 25°C, the amounts of Fe in amorphous oxides by acid-ammonium oxalate dissolution in the dark (Fe_O, Schwertmann, 1964). In the NH_4-oxalate extract Al was also determined (Al_O). The total element contents were determined by HF-HNO_3 dissolution (Bernas, 1968), on ignited (1000°C) samples. In all extracts the element contents were determined by AAS and all analyses were duplicated.

The clay fraction (< 2 µm) was separated by sedimentation for the mineralogical analyses, Mg saturated with $MgCl_2$, washed until free of Cl^-, and freeze-dried. The X-ray diffraction (XRD) analyses were carried out using a Philips PW1710 diffractometer (40kV and 20 mA, graphite monochromator) on air dried (AD), ethylene glycol solvated (EG), K-saturated (K) and heated (550°C) oriented mounts. Scans were made from 3 to 35 º2θ at a speed of 1 º2θ min^{-1}. The

presence of HIV was ascertained, and its thermo-stability assessed, by heating the K-saturated samples to 110, 335 and 550°C. When necessary, the fine clay fraction (<0.2 µm), was separated by centrifugation (30 min at 3000 rpm at 25°C in a 4227 RCF Meter refrigerated centrifuge), saturated with $MgCl_2$, washed until free of Cl^-, freeze-dried, and analysed by XRD as oriented mounts.

The sand fraction was separated by wet sieving after oxidation of organic matter with H_2O_2, and analysed as randomly oriented mounts from 3 to 80°θ, with the addition of 20% CaF_2 as internal standard. The intensity of the most intense peaks of quartz (0.334 nm), K-feldspars (0.324 nm), and plagioclases (0.318 nm) were thus compared with the intensity of the CaF_2 0.193 nm peak, to have an estimate of the trend of mineral abundance in the sands.

RESULTS

Profile morphology and chemical properties

The soils were classified according to the USDA Soil Taxonomy (Soil Survey Staff, 1999) as: Typic Cryaqualf at site 1, and Typic Glossocryalfs at sites 2 and 3. Organic horizons were always present, although they were more expressed at site 1, about 30-40 cm thick, composed of Oi, Oe and Oa. At sites 2 and 3, Oi and Oe horizons prevailed, but they were less thick (<10 cm). At the three sites, the Oa was mixed with the first mineral horizon. All three profiles showed the presence of Bt horizons, but only profiles 2 and 3 also presented the Bs horizon which is typical of podzolisation (Table 1). In profile 1 marked evidences of water stagnation were visible, with the presence of a Btg horizon. The eluvial horizon above the Bs was well expressed in profile 3, with a clear difference in colour, texture and structure, while profile 2 showed only the presence of a transitional E/A horizon. The Bt horizons were slightly thicker in profile 2 than in profile 3, and located deeper (Table 1). Below the Bt horizons a lithologic discontinuity was present in both profile 2 and 3. Clay migration

recognised in the field by the presence of clay cutans on the ped faces was confirmed by textural data, hence meeting the criteria for diagnostic argillic horizons (Table 1). The maximum enrichment in clay was found between 90 and 116 cm in profile 2, while it was at shallow depth in profile 3, between 25 and 40 cm.

The coarse sand content was high in the near surface horizons, decreased in the middle ones and, in profiles 2 and 3, increased again in the bottom horizons (Table 1). When the coarse sand content was determined after treating the soil samples with H_2O_2, the high amounts in the surface horizons were no more present, indicating a pronounced aggregation of silt and clay by organic matter in the upper horizons. The increase in coarse sand in the deepest horizons of profiles 2 and 3 was instead still visible, and confirmed the presence of the lithologic discontinuities evidenced in the field.

All soils had acidic reaction and showed organic matter concentrated in the near-surface horizons (Table 1). The C/N ratio was lower in profile 2, reflecting the different composition of vegetation cover. The CEC followed the organic matter trend ($r = 0.95$, $n = 23$, $p < 0.001$) and the base saturation abruptly increased in the bottom horizons.

In profile 1, marked variations in the contents of Fe were visible (Table 2). The AB horizons showed Fe depletion, both in the extractable (Fe_D and Fe_O) and in the total forms (Fe_T). Fe depletion was confirmed by the ratios between Si and Fe_T, which sharply decreased in the bottom horizons, while the Si to Al_T ratio showed less pronounced variations (Table 2). The NH_4-oxalate-extractable Al showed only small variations through the profile (Table 2). In profile 2, the Bs horizon showed the highest concentration of both NH_4-oxalate and DCB-extractable Fe; below it the amounts of iron oxides were relatively homogeneous with the exception of the bottom horizon (2BC). The Al_O showed the same trend of the Fe_O, with high contents in the Bs horizon. The Si/Al_T and Si/Fe_T ratios indicated a relative enrichment in metals with respect to Si in the top horizons, with very low values in the Bs. The 2BC horizon

showed higher ratios than the Bt ones. A depletion of all forms of Fe, including Fe_T, was visible in the Oa/E and E horizons of profile 3, followed by a relative increase in Bs. Both the Si/Al_T and Si/Fe_T ratios were rather high down to the Bs, then decreased, and increased again in the 2BC horizons, but the Si/Fe_T trend was more marked. An accumulation of NH_4-oxalate extractable Al also occurred in the Bs horizon.

Mineralogy

The main silicate minerals in the sand fractions were quartz and feldspars. Both K-feldspars and plagioclases were present, as evident from the peak at 0.324 nm and from the strong reflections in the range 0.318-0.322 nm (Brown, 1980). The ratios between the intensities of the peaks of these minerals in the sand and the CaF_2 peak at 0.193 nm are shown in Figure 2. In profile 1, no clear trend in the ratio between quartz and CaF_2 was found, while in the bottom horizons of profiles 2 and 3, a sharp increment was evident (Figure 2A). In addition, in profile 3, a relatively high content of quartz was found in the E1 horizon. Feldspars were not found in the first three horizons of profile 1 (Figure 2B and 2C), and the ratios were rather irregular in all profiles.

The clay fraction is composed of a complex suite of minerals in all samples. Kaolinite was however always present, together with illite.

In profile 1, the relative intensity of the kaolinite 0.7 nm peak in the untreated sample was generally higher in the upper part of the profile than in the bottom (Figure 3). In the clay fraction, feldspars were found in all horizons, even where they were not detected in the sand. A broad diffraction band between 1.4 and 1.0 nm indicated the presence of a random mixed layer illite-vermiculite or smectite, particularly abundant in the AB horizons. When the sample was EG solvated (Figure 3), the changes in the diffraction band between 1.4 and 1.0 nm indicated some swelling in these mixed layer minerals, except for the Btg horizon.

Vermiculite was abundant in the Bt1 and Btg horizons, as visible by comparing Figures 2 and 3. Upon heating to 550°C (Figure 4), some chlorite was also found, as a small peak at 1.4 nm remained, but only in traces in most horizons. In the Bt1 and Bt2 horizons the 1.4 nm peak intensity sharply decreased after heating the sample to 110°C, while it was necessary to reach 335°C in the case of Btg (Figure 4), indicating the presence of some Al polymers in the interlayer. When compared to the bulk clay, the fine clay fraction of all horizons evidenced a lower presence of illite and kaolinite and a relative increase of vermiculite (Figure 5). As almost no chlorite was present in these samples, the 1.4 nm peak after EG solvation was totally related to vermiculite. The slight swelling behaviour that was visible in the bulk clay fraction was no more present in the AB1, and AB2 horizons, while it was still evident in the two deepest horizons (Bt1 and Bt2).

In profile 2, the highest variability among horizons was related to mixed layer minerals. Irregularly interstratified illite-vermiculite or smectite was in fact present in all horizons, as visible in the 1.4-1.0 nm region of the spectra upon EG solvation, but the shape of the diffraction band suggested a variable proportion of the components (Figure 6), with more illite in the deepest horizons. In addition, the mixed layers did not show any swelling behaviour in the E/A, Bs and Bw horizons, while the shape of the diffraction band changed markedly upon EG solvation in the Bt and 2BC horizons (Figure 6). In the E/A horizon a marked collapse to 1.0 nm was observed after heating the mounts to 550°C, while the 1.0 nm peak was rather broad in the Bs horizon, suggesting the presence of HIV (Figure 7A). This was confirmed by heating the K-saturated samples; in the E/A horizon the peak collapsed to 1.0 nm at 335°C, while it was necessary to reach 550°C to obtain a 1.0 nm peak in the Bs (Figure 7A). In the Bt and 2BC horizons, the interlayering of Al polymers was less marked than in the Bs, although it was still present (Figure 7B), as the collapse to 1.0 nm was obtained after heating to 335°C. A shoulder was however still present towards the low angle

side of the 1.0 nm peak in the Bt horizons. Traces of chlorite were visible in all horizons, especially in the upper sequum.

In profile 3, the intensity of the 1.4 peak in the air-dry samples sharply decreased towards the bottom horizons, where an irregular 1.4-1.0 mixed layer predominated in the Bt2 and 2BC1 (Figure 8). In the air-dried 2BC2 sample instead, the 1.4 nm peak was again more evident. Swelling after EG solvation was evident in the three deepest horizons (Bt2, 2BC1 and 2BC2). No swelling was instead detected in the Bs and Bt1 horizons, but it was again present in the E horizons (Figure 8). Chlorite was present in traces in the E2, Bs and Bt1, while no peak at 1.4 nm was visible after heating in the other horizons (Figure 9A). The behaviour of the K-saturated samples after heating (Figure 9B) indicated the presence of hydroxyl-polymers in the interlayer in the B horizons: no collapse to 1.0 nm was obtained after heating to 110°C, and a shift towards the higher angles was visible at 335°. The shift was more marked in the Bt horizons than in the Bs, but it was always necessary to reach 550°C to obtain the complete collapse. In the 2BC horizons, the collapse to 1.0 nm was already obtained at 110°C.

DISCUSSION

Several combinations of pedogenic processes have acted on these profiles. Clay translocation was evident in all three profiles, combined with podzolisation in profiles 2 and 3, and symptoms of hydromorphism were present in profiles 1 and 3.

In profile 1 the gleyic properties were evident in the field, hence suggesting a strong weathering of the Fe-bearing minerals. This was confirmed by the chemical analyses, showing a depletion of all Fe forms in the top of the profile. The depletion in Fe oxides and hydroxides was particularly evident, but losses of Fe from silicates have also occurred, as evident by comparing the trends of the Si/Al_T and Si/Fe_T ratios. A phenomenon which is often caused by waterlogging is the removal of Fe-coatings from sand grains and mineral

surfaces (e.g. Favre et al., 2002). The presence of feldspars in the clay fraction and their absence in the sand strongly suggests a physical disintegration of the mineral grains upon freezing, probably promoted by the lack of protective Fe films dissolved by reducing conditions (Zeidelman, 1998). In the Btg horizon, the weathering of Fe-bearing phases was less striking, and the horizon appeared as a transition between the AB and the other Bt ones. The mobilisation of Fe forms has occurred, but only the secondary phases have been involved, as showed by the relatively high contents of Fe_T and the low ratio Fe_D/Fe_T.

Sharp differences in clay mineralogy between the AB and Bt horizons were visible and may be related to a pronounced weathering in the top of this profile, as pointed out by the disappearance of the 1.4 nm peak in the top horizon. As pedogenic kaolinite is typically found in warmer conditions and deeply leached environments (Allen and Hajek, 1989), its apparent higher content is probably the result of residual accumulation upon dissolution of the less stable 1.4 nm layer silicates. The organic acids released by Sphagnum may have acted on the 1.4 nm minerals by removing Al from the interlayer, when present, and from structural sites, thus enhancing mineral dissolution and causing a decrease in layer charge (April et al., 2004). In addition, organic acids also decrease of the activity of Al^{3+} and of Al-hydroxocomplexes in the soil solution (Drever and Stillings, 1997). The low activity of Al-hydroxocomplexes may be the responsible for the moderate formation of Al-interlayered minerals, which is better expressed in the other two profiles. A pronounced weathering in the surface horizons is also in agreement with the presence of a swelling component in the mixed layers, which is probably the result of the weathering of illite followed by charge reduction, as supported by its absence in the fine clay fraction, and often reported in other soils of that area (Sokolova et al., 2001). Also from the mineralogical point of view the Btg reflects the transition between the AB horizons and the other Bt ones: the vermiculite phase became more important, but kaolinite was still a major component of the clay fraction. This was the only horizon of this

profile where swelling was not detected, thus suggesting a different origin of the smectitic components found in the AB and Bt horizons. In the deepest Bt horizons, smectite may be preserved because of the high concentration of base cations, and of a low weathering intensity, as indicated by low relative contents of kaolinite in the clay fraction and the high amounts of feldspars in the sand.

In profiles 2 and 3, podzolisation was evident in the upper part of the profile and clay migration in the lower one. These processes have acted with different intensities in the two profiles and, in the upper sequum of profile 3, some reduction processes have also occurred.

In both profile 2 and profile 3 a lithologic discontinuity was located immediately below the Bt horizons; it may have thus altered water flow and favoured the clay deposition, as pointed out by Bockheim (2003). However, the maximum enrichment in clay in profile 3 was situated well above the discontinuity, suggesting that clay migration has been less intense than in profile 2, where the maximum clay content was located deeper, immediately above the discontinuity.

In the horizons of the lower sequa of profiles 2 and 3, the layer silicates showed the transformations that are expected in Alfisols and the variations in the composition of the illite-vermiculite mixed layers pointed towards the vermiculitisation of illite. In both profiles, the pH of the Alfisol sequa favours Al immobilisation and Al-hydroxomonomers may have been incorporated in the interlayer of vermiculite, as found by Bain et al. (1990) in some acid soils of Scotland. The Al intercalation was present in the Bt of both profiles, as the collapse to 1.0 nm was obtained only after heating, but the profiles were different below the discontinuity. HIV was present in profile 2, indicating that the translocation of clay has transgressed the discontinuity; in profile 3 the 1.4 nm components showed a good collapse when K saturated, even at a room temperature. These results are in agreement with the higher intensity of the clay illuviation process in profile 2 deduced from profile morphology.

Although the process of podzolisation was clearly discernible from profile morphology and from the increase in Al_O and Fe_O in the Bs horizons of both profiles 2 and 3, it was not expressed enough to allow the soils to be classified as Spodosols. For the taxonomic placement of a soil into the Spodosol order the spodic index, calculated as $0.5Fe_O + Al_O$ (in %), must be greater than 0.5, and at least twice in the Bs with respect to the E horizon. In both profiles, the differences between eluvial and illuvial horizons were not sharp enough, and, in addition, in profile 3 the spodic index did not reach the threshold value. In this profile however the upper sequum showed also some symptoms of hydromorphic conditions, although less marked than in profile 1. This additional process might lead to an underestimate of the intensity of podzolisation.

In profile 2, where no waterlogging has occurred, the effect of podzolisation on mineral transformations was visible. The podzolisation process was effective in Fe mobilisation from the primary phases, thus inducing higher Fe_D/Fe_T ratios than in the Alfisol sequum; the high concentration of oxalate extractable-Fe testifies the immobilisation of organo-mineral complexes, as expected in Bs horizons (e.g. McKeague et al., 1983). Podzolisation was not particularly effective on the weathering of the layer silicates: traces of chlorite were present and no swelling minerals were found in the E and Bs horizons. The behaviour upon K-saturation and heating, indicative of the presence of HIV, showed however differences between the clay fraction of the Bs and that of the eluvial horizon, with a more marked Al-intercalation in the Bs than in the E/A horizon. By comparing the temperatures needed to obtain a complete collapse in all horizons of profile 2, the following sequence of Al-intercalation was visible: E/A ≈ 2BC < Bt < Bs. Thus, the vermiculite in the Bs was enriched in Al with respect to all other horizons. Mirabella and Sartori (1998) reported that the first weathering step in some Alpine podzols is the transformation of chlorite into HIV or HIS, followed by the removal of Al from the interlayer. In these Taiga soils, a mixed layer with

HIV has formed during Alfisol development, therefore, when podzolisation has started, the organic acids in the E horizons have probably complexed Al, and removed it completely from the interlayer. When the Al-organic complex is decomposed, thanks to the rather abundant microbial population in the soils of the study area (Golovchenko et al., 2000), the higher pH in the Bs horizon (5.0) may have favoured the precipitation of Al in the interlayer. A process that has begun during Alfisol formation is therefore continuing, further enriching the HIV component.

In the upper sequum of profile 3, an intense podzolisation is suggested by the presence of well defined eluvial horizons, as evident from the morphological data, and by the enrichment in quartz of the sand fraction in the E horizon. Quartz enrichment can also be caused by the dissolution of weatherable primary minerals, but no such trend was found in the AB horizons of profile 1, where feldspars were no more present. However, as the accumulation of Al_O in the Bs was lower than that of Fe_O, the Fe increase in the Bs could also be related to the mobilisation of iron in reducing conditions and to its oxidation upon an increase in Eh. The lower Fe_D/Fe_T ratio than in profile 2 suggests, in fact, that the formation of secondary Fe phases has not completely impeded Fe depletion, and while the Si to Al_T ratio was comparable to profile 2, the Si/Fe_T was much higher, indicating the occurrence of reducing conditions.

The mineralogy of the clay fraction in E and Bs horizons was therefore the result of the combined effects of reducing conditions and podzolisation. Swelling mixed layers were found in the E horizons of profile 3, although there were not present in the eluvial horizon of profile 2, further suggesting that a more intense weathering has occurred in the upper sequum of profile 3, compared to profile 2. In Bs horizon of profile 3, swelling mixed layers were not present, either because of Al intercalation in the interlayer after decomposition of the organic-Al complexes, or because of charge increase upon waterlogging (e.g. Gates et al., 1993,

1998). The horizons where gleying was more intense were the E horizons, and there, swelling was detected. A lack of swelling in the Bs horizon caused by Fe reduction can therefore be excluded. Furthermore, another transformation which is frequently observed in waterlogged soils is the enhancement of K fixation in the interlayer (Chen et al., 1987), coupled with an increase in CEC (e.g. Favre et al., 2002). Our data showed that, upon K-saturation, the collapse to 1.0 nm was more evident in the E horizons than in the Bs. The clay mineral transformations observed in the upper sequum of profile 3 seem therefore those typically associated to the process of podzolisation, and, as in profile 2, they have occurred to clay minerals formed during the previous pedogenic process.

The moderate expression of podzolisation, in terms of accumulation of Al and Fe in the Bs horizons, could be related to marked losses of these elements, with multiple causes acting together. In the case of Al, the intercalation into the interlayers of phyllosilicates was probably coupled with lateral movements of water, which are widespread in the study area, and have been documented since the fifties (Vasiliev, 1950; Simonov, 1991). This phenomenon involves Al and Fe-organic complexes and is well kown for forest soils, where translocation of elements and podzolisation may occur not only vertically through the profile, but also laterally (Sommer et al., 2000; 2001).

CONCLUSIONS

In these studied soils, several pedogenic processes have occurred and the transformations of the clay fraction have been influenced to a large extent. During the formation of the Alfisol sequum, the expected transformation of illite into vermiculite or smectite through the formation of mixed layers has occurred, and Al-intercalation was favoured. When podzolisation started, these clay minerals were subjected to further transformations, driven by the presence of organic acids and to some extent by water stagnation at the top of the profile.

In the podzolic sequum the presence of HIV/HIS in the E horizon was no longer favoured, but in the Bs horizons Al-intercalation in the interlayers continued, thus prolonging a mineralogical process that has started during Alfisol formation. The reducing conditions which were also present in the area acted upon soil minerals, but affected directly only Fe oxi(hydr)oxides. The dissolution of the protective Fe-films from mineral surfaces has however favoured the physical disintegration of feldspar grains where waterlogging was present. The well known formation of swelling minerals in podzols was only moderately visible and related to the cheluviation phase. Swelling behaviour was in fact not visible in the podzol sequum where the vegetation cover was an admixture of conifers and broadleaves. It was instead present both where spruce was dominant and the weathering intensity in the E horizons was higher, and where a thick sphagnum cover has developed because of hydromorphic conditions.

ACKNOWLEDGMENTS

This research was funded by INTAS (project n. 2001-0512) and by the EU (INCO-DC-013388, OMRISK).

REFERENCES

Allen, B.L. and Hajek, B.F., 1989 Mineral occurrence in soil environments. In: J.B. Dixon and S.B. Weed (Editors), Minerals in soil environments. Soil Science Society of America, Madison, Wisconsin. pp. 199-278

April, R.H., Keller, D. and Driscoll, C.T., 2004. Smectite in Spodosols from the Adirondack Mountains of New York. Clay Minerals, 39: 99-103.

Arocena, J.M. and Sanborn, P., 1999. Mineralogy and genesis of selected soils and their implications for forest management in central and Northeastern British Columbia. Canadian Journal of Soil Science, 79: 571-592.

Bain, D.C. and Duthie, D.M.L., 1984. The effect of weathering in the silt fractions on the apparent stability of chlorite in Scottish soil clays. Geoderma, 34: 221-227.

Bain, D.C., Mellor, A. and Wilson, M.J., 1990. Nature and origin of an aluminous vermiculitic weathering product in acid soils from upland catchments in Scotland. Clay Minerals, 25: 467-475.

Banfield, J.F. and Murakami, T., 1998. Atomic-resolution transmission electron microscope evidence for the mechanism by which chlorite weathers to 1:1 semiregular chlorite-vermiculite. American Mineralogist, 83: 348-357.

Bernas, B., 1968. A new method for decomposition and comprehensive analysis of silicates by atomic absorption spectrometry. Analytical Chemistry, 40: 1682-1686.

Bockheim, J.G., 2003. Genesis of bisequal soils on acidic drift in the upper great lakes region, USA. Soil Science Society of America Journal, 67: 612-619.

Brown, G., 1980. Associated minerals. In: G.W. Brindley and G. Brown (Editors), Crystal structures of clay minerals and their X-ray identification. Monograph 5, Mineralogical Society, London, pp. 361-410.

Chen, S.Z., Low, P.F. and Roth, C.B., 1987. Relation between potassium fixation and the oxidation state of octahedral iron. Soil Science Society of America Journal, 51: 82-86.

Chesworth, W., 1992. Weathering systems. In: I.P. Martini and W. Chesworth (Editors), Weathering, soils and paleosols. Elsevier, Amsterdam, pp. 19-40.

Churchman, G.J., 1980. Clay minerals formed from micas and chlorites in some New Zealand soils. Clay Minerals, 15: 59-76.

David, M.B. and Vance, G.F., 1991. Chemical character and origin of organic acids in streams and seepage lakes of Central Maine. Biogeochemistry, 12: 17-41.

Deckers, J.A., 2001. Albeluvisols. In: Lecture notes on the major soils of the world. FAO, Rome.

Drever, J.I. and Stillings, L.L., 1997. The role of organic acids in mineral weathering. Colloids and Surfaces A: Physicochemical and Engineering Aspects, 120: 167-181.

Egli, M., Mirabella, A., Sartori, G. and Fitze, P., 2003. Weathering rates as a function of climate: results from a climosequence of the Val Genova (Trentino, Italian Alps). Geoderma, 111: 99-121.

Egli, M., Mirabella, A., Mancabelli, A. and Sartori, G., 2004. Weathering of soils in Alpine areas as influenced by climate and parent material. Clays and Clay Minerals, 52: 287-303.

Favre, F., Tessier, D., Abdelmoula, M., Génin, J.M., Gates, W.P. and Boivin, P., 2002. Iron reduction and changes in cation exchange capacity in intermittently waterlogged soils. European Journal of Soil Science, 53: 175-183.

Gates, W.P., Wilkinson, H.T. and Stucki, J.W., 1993. Swelling properties of microbially reduced ferruginous smectite. Clays and Clay Minerals, 41: 360-364.

Gates, W.P., Jaunet, A., Tessier, D., Cole, M.A., Wilkinson, H.T. and Stucki, J.W., 1998. Swelling and texture of iron-bearing smectites reduced by bacteria. Clays and Clay Minerals, 46: 487-497.

Gee, G.W. and Bauder, J.W., 1986. Particle-size analysis. In: A. Klute (Editor), Methods of soil analysis, Part 1, 2nd Edition. Agronomy Monograph 9, Agronomy Society of America and Soil Science Society of America, Madison, Wisconsin, pp. 383-411.

Golovchenko, A.V., Dobrovoi'skaya, T.G., Maksimova, I.A., Terekhova, V.A., Zvyagintsev, D.G. and Trofimov, S. Ya., 2007. Structure and role of microbial communities in Southern Taiga Soils. Microbiology, 69: 371-380.

Kitagawa, Y., 2005. Characteristics of clay minerals in podzols and podzolic soils. Soil Science and Plant Nutrition, 51: 151-158.

McKeague, J.A., DeConinck, F. and Franzmeier, D.P., 1983. Spodosols. In: L.P. Wilding, N.E. Smeck and G.F. Hall (Editors), Pedogenesis and soil taxonomy. II: The soil orders. Elsevier, Amsterdam, pp. 217-252.

Mehra, O.P. and Jackson, M.L., 1960. Iron oxide removal from soils and clays by a dithionite-citrate system buffered with sodium bicarbonate. Clays and Clay Minerals. Proceedings of the 7th National Conference on Clays and Clay Minerals. Oct. 20-23, 1958, Washington, D.C.

Mirabella, A. and Sartori, G., 1998. The effect of climate on the mineralogical properties of soils from the Val Genova valley – Trentino (Italy). Fresenius Environmental Bulletin, 7 (5a-6a): 478-483.

Puzachenko, Yu.G., Zheltukhin, A.S., Kozlov, D.N., Korablev, N.P., Fedyaeva, M.V., Puzachenko, M.Yu and Siunova, E.V., 2007. Central Forest State Biosphere Reserve. Delevoi Mir Publisher, Moscow (in Russian)

Rhoades, J.D., 1982. Cation Exchange Capacity. In: A.L. Page, R.H. Miller and D.R. Keeney (Editors), Methods of Soil Analysis, part 2, 2nd edition. American Society of Agronomy, Madison, Wisconsin, pp. 149-157.

Righi, D., Huber, K. and Keller, C., 1999. Clay formation and podzol development from postglacial moraines in Switzerland. Clay Minerals, 34: 319-332.

Robert, M. and Berthelin, J., 1986. Role of biological and biochemical factors in soil mineral weathering. In: P.M. Huang and M. Schnitze (Editors), Interactions of soil minerals with natural organics and microbes. Special Publication 17, Soil Science Society of America, Madison, Wisconsin, pp. 453-495.

Ross, G.J., 1969. Acid dissolution of chlorites: release of magnesium, iron and aluminium and mode of acid attack. Clays and Clay Minerals, 17: 347-354.

Schwertmann, U., 1964. Differenzierung der Eisenoxide des Bodens durch Extraktion mit Ammoniumoxalat-lösung. Zeitschrift für Pflanzenernhärung, Düngung und Bodenkunde, 105: 194-201.

Simonov, G.A., 1991. Detailed study of morphological variability of podzolic soils in the Middle Taiga. In: S.V. Zonn (Editor), Degradation and recovery of Forest Soils. Nauka Publications, Moscow, pp. 235-243 (in Russian).

Soil Survey Staff, 1999. Soil Taxonomy, A basic system of soil classification for making and interpreting soil surveys. 2nd edition. Agriculture Handbook 436, Natural Resources Conservation Service, U.S. Govt. Printing Office, Washington, D.C.

Sokolova, T.A., Dronova, T.Ya., Tolpeshta, I.I. and Ivanova, S.E., 2001. Interaction of Forest Podzolic Soils with Model Acid Precipitation and Acid-Base Buffering Capacity of Podzolic Soils. Publishing House of Moscow State University, Moscow (in Russian).

Sommer, M., Halm, D., Weller, U., Zarei, M. and Stahr, K., 2000. Lateral podzolization in a granite landscape. Soil Science Society of America Journal, 64: 1434-1442.

Sommer, M., Halm, D., Geisinger, C., Andruschkewitsch, I., Zarei, M. and Stahr, K., 2001. Lateral podzolization in a sandstone catchment. Geoderma, 103: 231-247.

Środoń, J., 1999. Nature of mixed-layer clays and mechanisms of their formation and alteration. Annual Review of Earth and Planetary Sciences, 27: 19-53.

Stucki, J.W., 2006. Properties and behaviour of iron in clay minerals. In: F. Bergaya, B.K.G. Theng and G. Lagaly (Editors), Handbook of clay science. Elsevier, Amsterdam, pp. 423-475.

Vasiliev, I.S., 1950. Moisture Regime of Podzolic Soils. Proceedings of the Dokutchaev Soil Science Institute 31, Academy of Sciences of the USSR Publisher, Moscow – Leningrad (in Russian).

Wilson, M. J., 2004. Weathering of the primary rock-forming minerals: processes, products and rates. Clay Minerals, 39: 233-266.

Zaidelman, F.R., 1998. The process of gleyfication and its roles in soil formation. Publishing House of Moscow State University, Moscow (in Russian).

Table 1: Selected morphological and chemical characteristics of the soil profiles

Profile	Horizon	Depth	Limits[1]	Colour[2]	Texture[3]	Structure[4]	CSa[5]	FSa	Silt	Clay	CSa H2O2	pH	C	C/N	CEC	Ca	Mg	K
		cm					----------%----------						g kg^{-1}		----------$cmol_c$ kg^{-1}----------			
Profile 1 Typic Cryaqualf	Oa/A	0-13	cw	10YR3/3	ls	f1gr	45.7	32.1	20.9	1.2	1.3	4.0	212.9	24.6	62.4	1.48	0.72	0.23
	AB1	13-25	cw	10YR4/3	sl	f1sbk	1.3	46.6	46.9	5.2	0.2	4.8	87.7	41.0	12.2	0.20	0.06	0.03
	AB2	25-37	ci	10YR5/3	sil	vf1sbk	0.4	37.7	53.9	8.1	0.1	4.4	13.1	40.0	8.7	0.14	0.07	0.05
	Btg	37-46	cw	5Y5/2	l	m2sbk	0.6	38.6	49.3	11.5	0.1	4.8	3.4	28.2	8.2	0.39	0.28	0.09
	Bt1	46-68	cs	10YR6/4	sil	c2abk	1.1	34.9	51.3	12.5	0.1	4.9	2.5	27.2	8.9	0.92	0.69	0.21
	Bt2	68-105+	--	10YR6/4	l	vc3abk	1.1	44.4	45.0	9.5	0.3	5.6	1.4	31.7	8.1	1.70	1.07	0.08
Profile 2 Typic Glossocryalf	Oa/E	0-3	cw	5YR4/1	sl	vf1sbk	28.1	35.4	32.9	3.6	0.8	4.2	72.4	19.8	25.7	0.16	0.25	0.08
	E/A	3-17	cw	5YR5/2	sl	f1gr	24.5	43.2	29.9	2.4	0.5	4.7	48.8	16.8	22.6	0.36	0.20	0.06
	Bs	17-35	ci	5YR4/3	sl	vf1gr	19.2	32.3	46.5	2.0	0.4	5.0	17.2	14.9	15.4	0.86	0.05	0.05
	Bw	35-45	cw	5YR5/4	sil	f1sbk	5.4	33.6	57.8	3.2	0.1	4.8	3.4	18.7	7.4	0.14	0.02	0.02
	Bt1	45-50	cs	7.5YR5/4	sil	f2abk	3.1	30.6	59.7	6.7	0.2	4.9	1.4	20.7	7.5	0.06	0.05	0.04
	Bt2	50-70	cs	7.5YR5/6	sil	m3abk	2.4	38.6	50.3	8.7	0.3	4.7	0.9	11.5	8.1	0.17	0.16	0.06
	Bt3	70-90	cw	7.5YR5/6	l	c3abk	1.9	49.0	40.9	8.3	0.1	5.2	0.6	16.5	6.3	0.52	0.20	0.05
	Bt4	90-116	cs	7.5YR4/6	l	c3abk	2.0	44.6	43.2	10.2	0.2	5.3	0.6	11.6	8.1	1.05	0.38	0.08
	2BC	116-133+	--	7.5YR 5/8	ls	vc2abk	20.4	63.5	11.3	4.9	17.1	5.4	0.4	32.9	4.6	0.55	0.26	0.06
Profile 3 Typic Glossocryalf	Oa/E	0-2	ai	10YR4/2	sl	vf1sbk	23.2	36.5	37.0	3.3	2.4	4.2	43.7	31.4	17.5	0.30	0.23	0.07
	E1	2-5	cw	10YR7/2	sil	f1sbk	10.1	31.4	52.4	6.3	0.4	4.1	12.6	30.9	12.5	0.10	0.06	0.06
	E2	5-10	cw	7.5YR7/2	sil	m2sbk	6.7	27.3	59.3	6.7	0.2	4.2	6.6	28.8	9.3	0.07	0.03	0.03
	Bs	10-25	cs	7.5YR6/4	sil	fmsbk	6.1	27.0	61.0	5.9	0.2	4.4	3.8	38.0	8.9	0.06	0.02	0.03
	Bt1	25-40	cw	7.5YR5/6	sil	f3abk	2.5	26.4	57.7	13.5	0.1	4.6	2.0	19.4	10.3	0.20	0.10	0.05
	Bt2	40-90	cs	7.5YR5/4	l	m3abk	2.1	41.3	48.8	7.9	0.2	5.2	0.5	15.5	8.6	2.03	1.05	0.09
	2BC1	90-100	cs	7.5YR5/8	ls	vc2abk	11.3	67.8	15.2	5.7	10.0	5.6	0.3	16.0	6.5	1.55	0.74	0.05
	2BC2	100-130+	--	7.5YR5/8	ls	c2abk	12.1	72.5	9.1	6.3	8.6	5.6	0.4	14.1	6.5	1.70	0.79	0.06

[1] distinctness - a: abrupt, c: clear; surface topography - s: smooth; w: wavy; i: irregular [2] Munsell notation for crushed dry soil material [3] ls: loamy sand, sl: sandy loam, l: loam, sil: silt loam [4] size – vf: very fine, f: fine, m: medium, c: coarse, vc: very coarse; grade - 1: weak, 2: moderate, 3: strong; type - gr: granular, abk: angular blocky, sbk: subangular blocky [5] CSa: coarse sand (2-0.2 mm); FSa: fine sand (0.2-0.05 mm); CSa_{H2O2}: coarse sand after oxidation with H_2O_2

Table 2: Al and Fe extractions and total SiO_2 contents in the soil profiles

	Al_O§	Fe_O	Fe_D	Fe_T	Fe_O/Fe_D	Fe_D/Fe_T	SiO_2	Si/Al_T	Si/Fe_T
		----------g kg^{-1}----------					%		
				Profile 1 (Typic Cryaqualf)					
Oa/A	2.53	0.53	0.80	8.12	0.66	0.10	85.82	18.37	31.80
AB1	1.35	0.05	0.08	10.22	0.69	0.01	89.22	20.58	48.78
AB2	1.14	0.07	0.09	8.23	0.73	0.01	88.77	18.86	61.19
Btg	1.03	0.93	1.09	15.59	0.85	0.07	86.39	15.60	32.39
Bt1	1.04	6.83	12.63	23.89	0.54	0.53	84.46	14.59	20.41
Bt2	1.01	2.05	9.10	19.04	0.23	0.48	85.93	16.72	26.19
				Profile 2 (Typic Glossocryalf)					
Oa/E	1.34	4.70	6.93	14.81	0.68	0.47	86.89	17.64	29.76
E/A	1.91	6.40	8.85	15.95	0.72	0.55	86.48	16.78	28.76
Bs	4.75	7.25	10.35	17.96	0.70	0.58	85.94	15.40	27.38
Bw	1.87	2.38	5.05	15.19	0.47	0.33	87.08	17.85	33.72
Bt1	0.93	2.50	5.10	15.66	0.49	0.33	87.62	18.53	33.63
Bt2	0.87	2.90	5.93	17.43	0.49	0.34	86.87	18.13	30.70
Bt3	0.58	2.80	5.80	17.56	0.48	0.33	87.26	18.59	30.86
Bt4	0.67	3.30	7.25	19.71	0.46	0.37	86.13	16.43	27.15
2BC	0.35	1.25	3.98	11.04	0.31	0.36	90.64	25.82	48.81
				Profile 3 (Typic Glossocryalf)					
Oa/E	0.96	1.20	1.38	8.03	0.87	0.17	90.47	22.89	62.59
E1	0.94	1.25	1.56	10.49	0.80	0.15	88.73	21.01	52.80
E2	0.66	1.91	2.70	9.52	0.71	0.28	89.78	21.45	59.71
Bs	0.97	3.15	4.60	13.80	0.68	0.33	88.69	20.05	41.26
Bt1	0.72	3.70	6.30	19.45	0.59	0.32	87.16	17.92	29.02
Bt2	0.39	2.38	6.50	17.86	0.37	0.36	87.54	19.01	31.18
2BC1	0.19	1.45	4.15	9.94	0.35	0.42	91.27	26.71	60.91
2BC2	0.26	1.50	4.20	11.52	0.36	0.36	91.30	27.69	52.77

§ Fe_O and Al_O: Acid ammonium oxalate extractable Fe and Al (Schwertmann, 1964); Fe_D: Na dithionite-citrate-bicarbonate extractable Fe (Mehra and Jackson, 1962); Fe_T: Total Fe

Figure 1: The study area

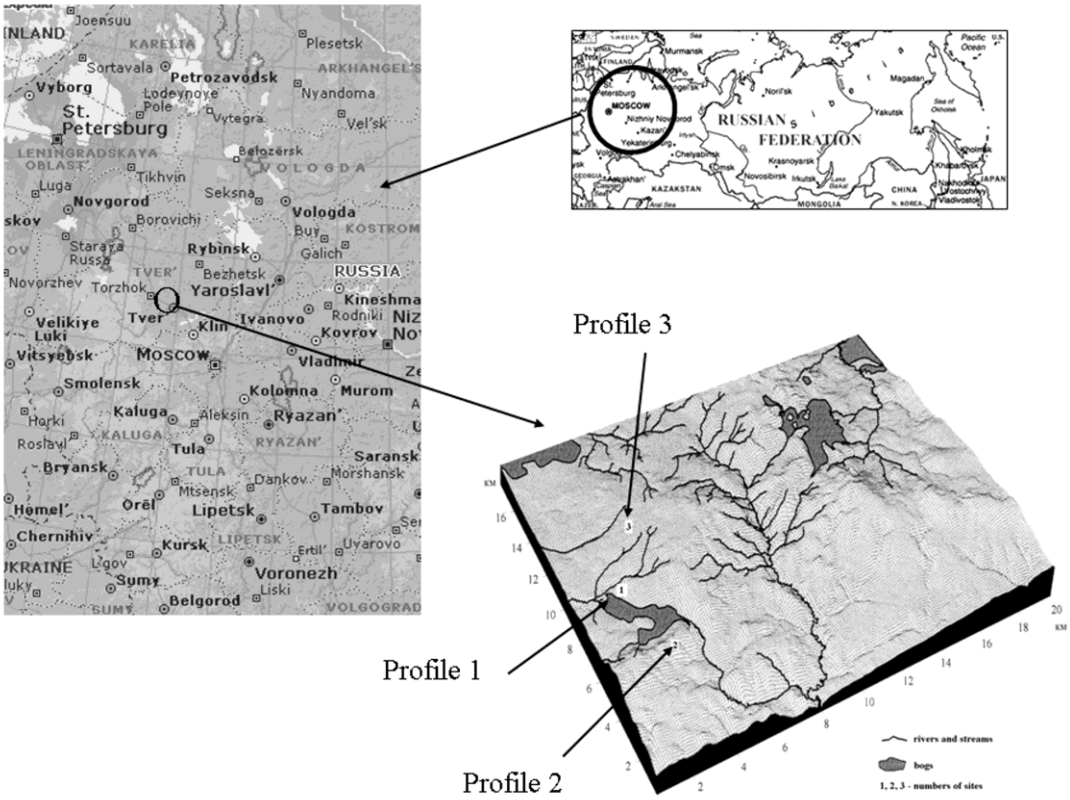

Figure 2: Ratios between the intensity of the peaks of quartz (0.331 nm, A), K-feldspars (0.324 nm, B) and plagioclases (0.318 nm, C), and the 0.193 peak of CaF_2. For graphical reasons, the horizons of Profile 1 are shown only in figure A, those of Profile 2 in B, and those of Profile 3 in C.

Figure 2

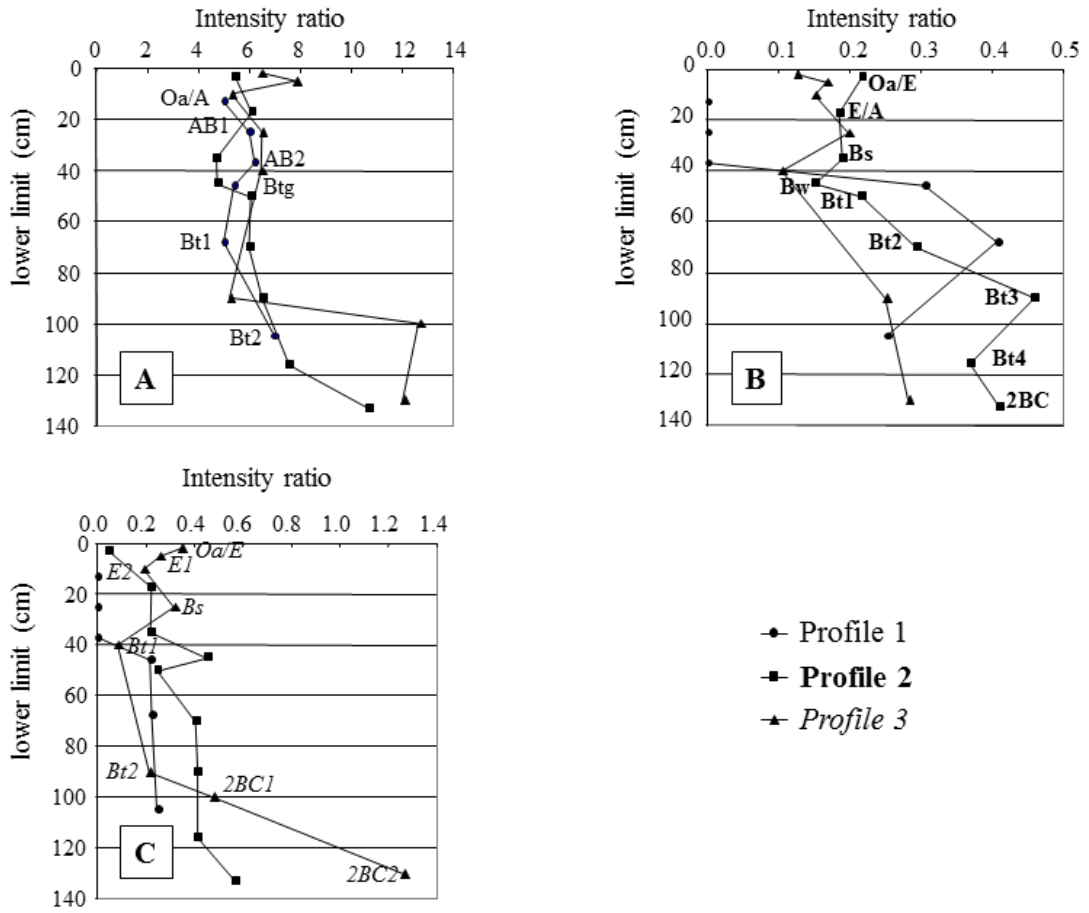

Figure 3: XRD patterns of the bulk clay fraction from Profile 1 after air-drying (AD) and ethylene-glycol solvation (EG)

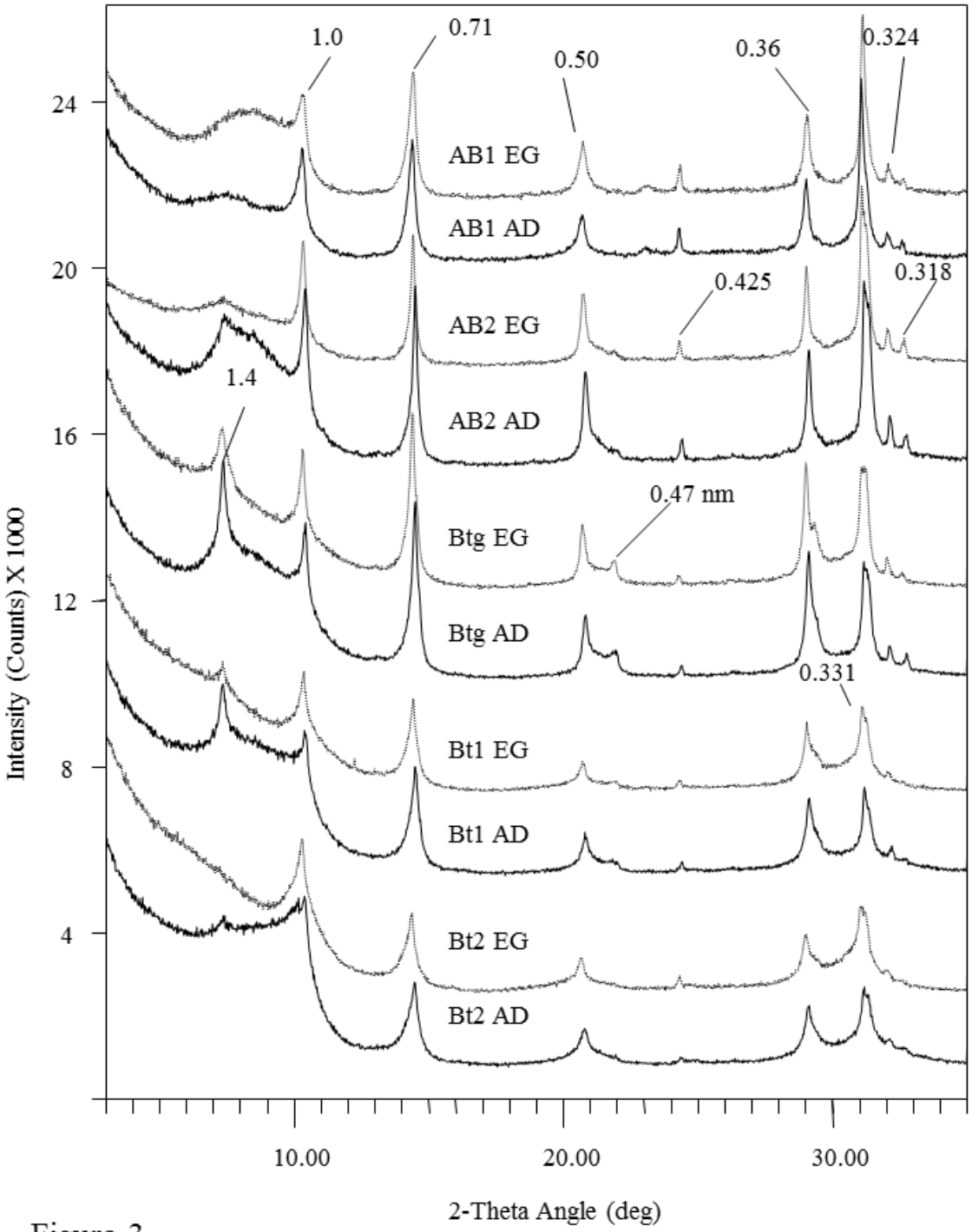

Figure 3

Figure 4: XRD patterns of the bulk clay fraction from Profile 1 after K-saturation and heating.

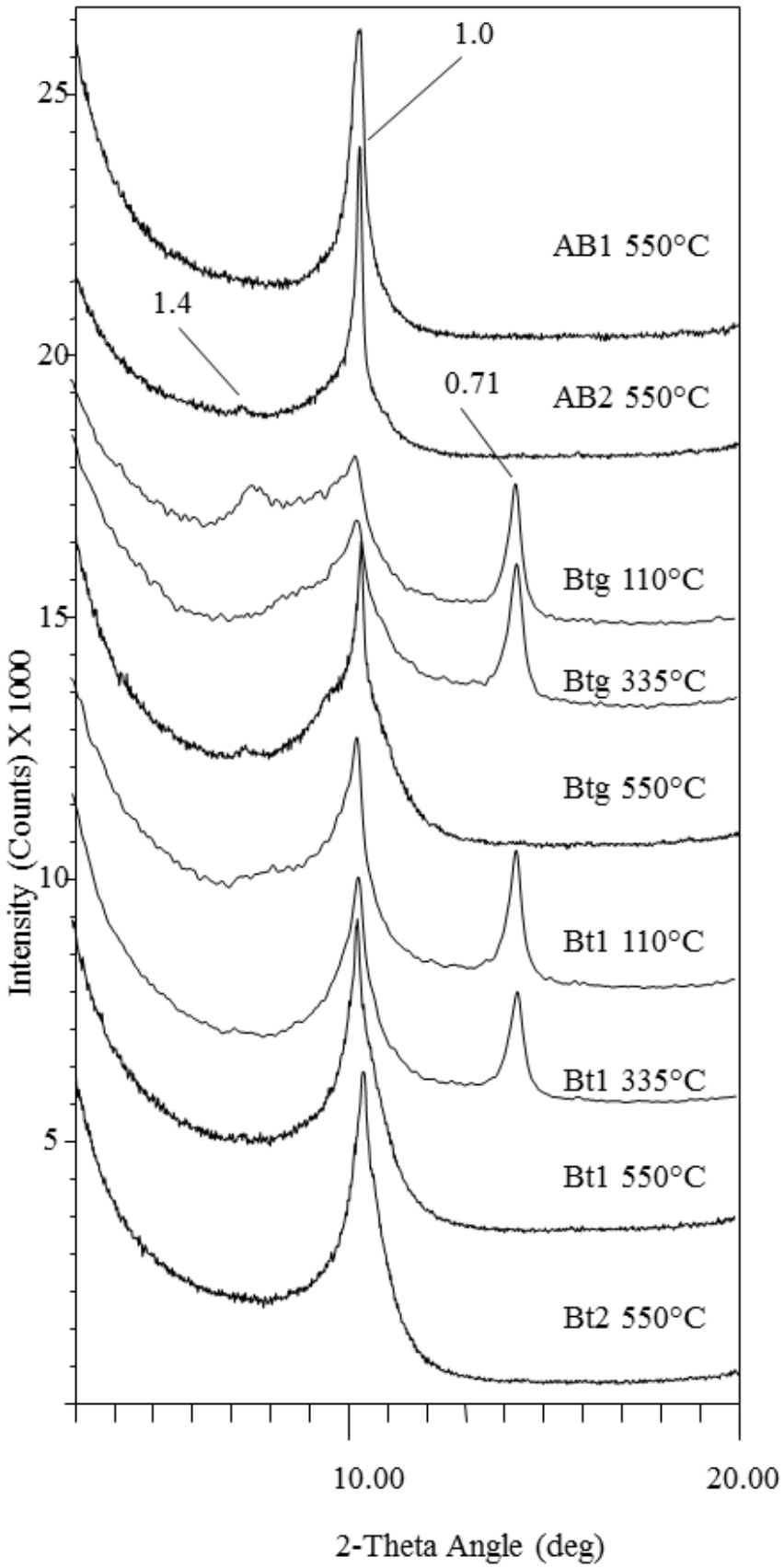

Figure 4

Figure 5: XRD patterns of the fine clay fraction from Profile 1 after air-drying (AD) and ethylene-glycol solvation (EG).

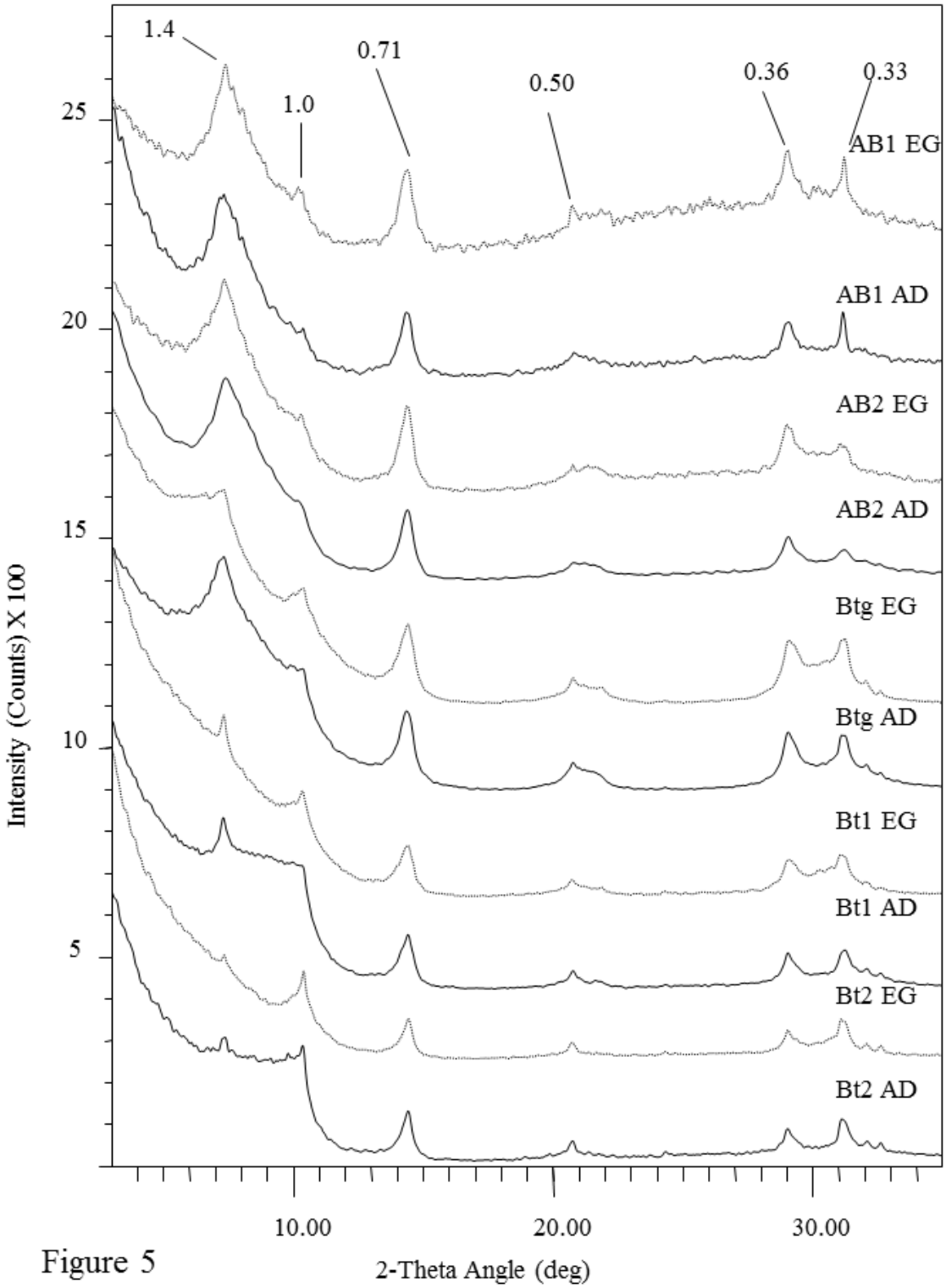

Figure 5

Figure 6: XRD patterns of the bulk clay fraction from Profile 2 after air-drying (AD) and ethylene-glycol solvation (EG)

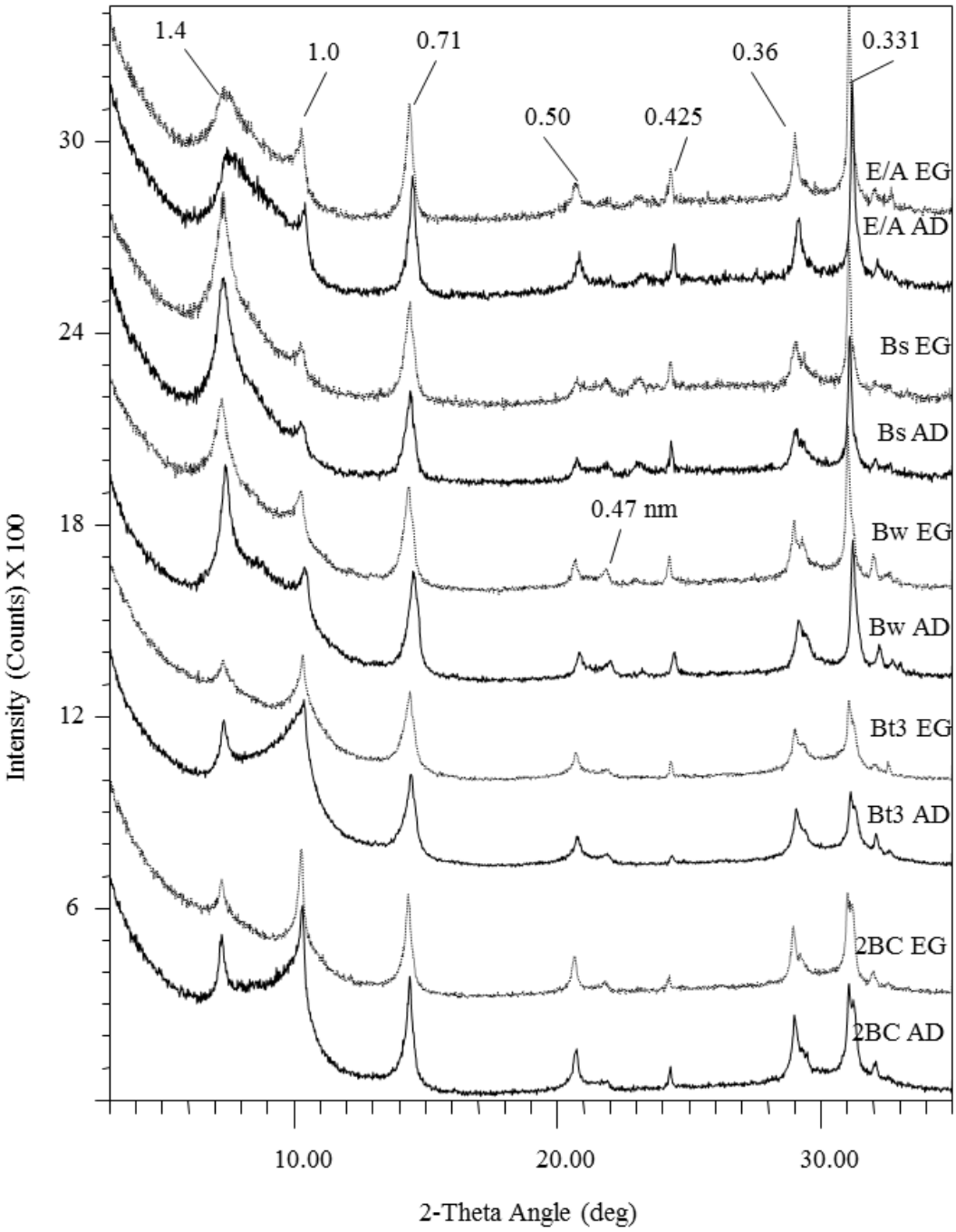

Figure 6

Figure 7: XRD patterns of the bulk clay fraction from the upper (A) and lower (B) sequum of Profile 2, after K saturation and heating.

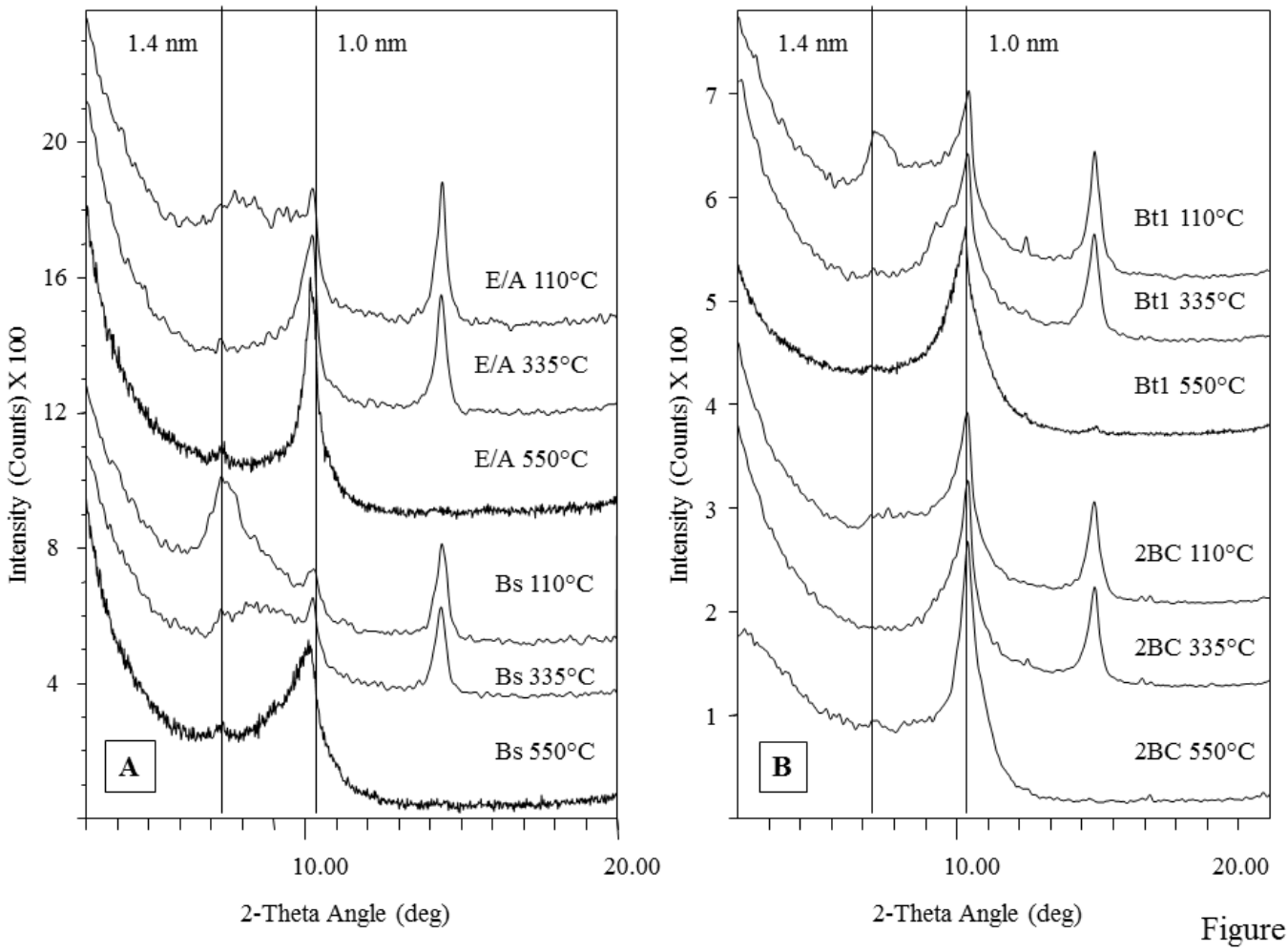

Figure 8: XRD patterns of the bulk clay fraction from Profile 3 after air-drying (AD) and ethylene-glycol solvation (EG)

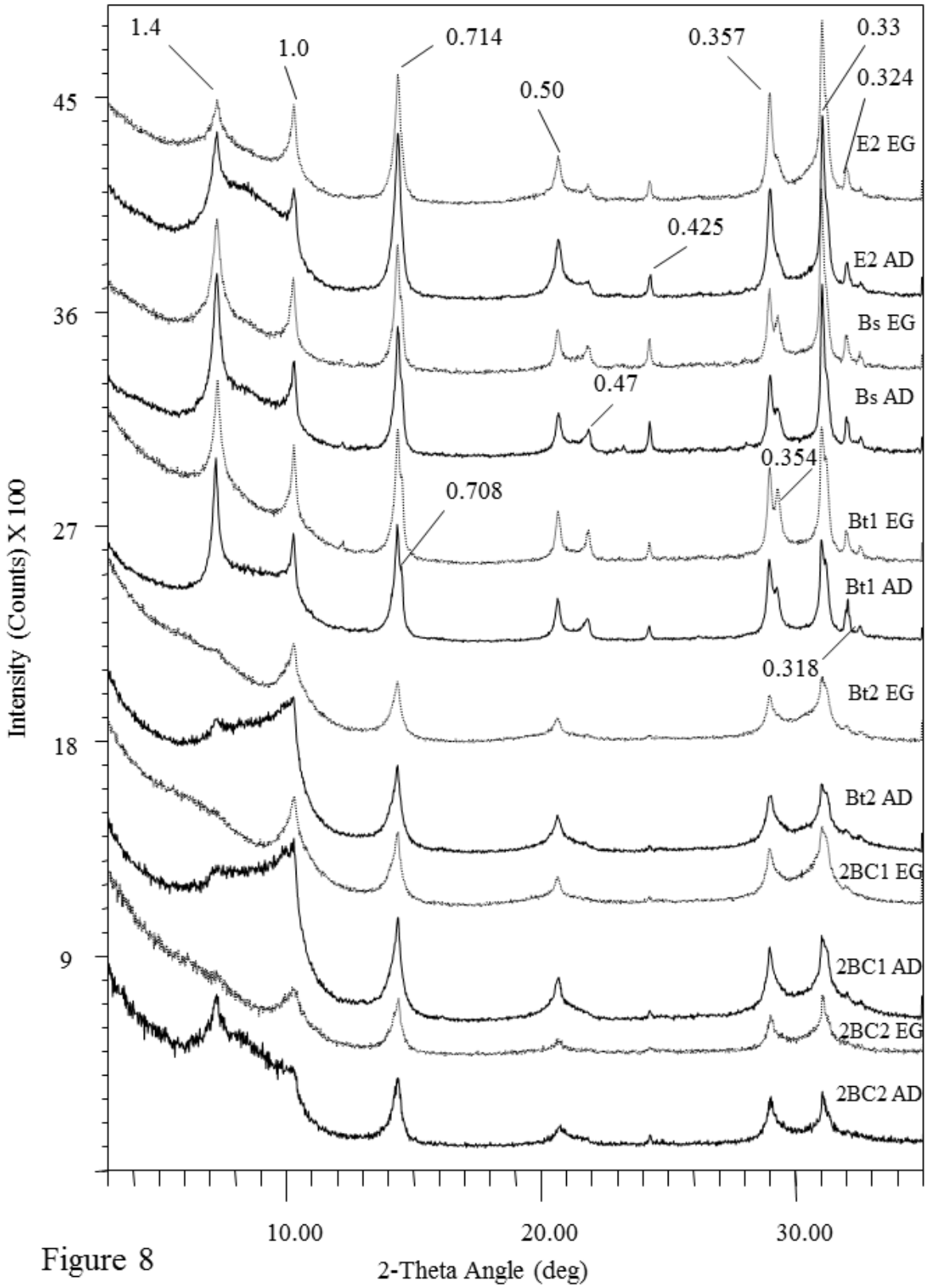

Figure 8

Figure 9: XRD trances of the bulk clay fraction from selected horizons of Profile 3 after heating to 550°C (A) and to lower temperatures (B)